WTC2005-63397

ANALYSIS OF GAS FOIL BEARINGS WITH PIECEWISE LINEAR ELASTIC SUPPORTS

Tae Ho Kim, Luis San Andrés
Mechanical Engineering Department, Texas A&M University,
College Station, Texas 77843-3123, USA

ABSTRACT

Gas foil bearings (GFBs) rely on their underlying elastic foundation to support radial loads at high rotor speeds. The bump foil strip compliance determines the maximum load capacity with large rotor excursions, well in excess of the bearing nominal clearance. GFBs must be designed properly to permit their reliable (predictable) usage in aircraft engines and other heavy load applications because an elastic foundation that is too soft results in a limited load capacity. Configurations in practical use include a second bump-strip layer or stop-pins underneath the original bumps which become active above a certain load threshold. In these last configurations, the overall stiffness of the support structure has piecewise load versus deflection characteristics. Presently, a simple physical model for GFBs with piecewise linear elastic supports follows. The analysis couples the Reynolds equation for the thin film flow of an ideal gas to the elastic supports motion. An exact flow advection model is adopted to solve the partial differential equations for the zeroth- and first- order pressure fields, thus rendering the GFB load capacity and frequency dependent rotordynamic force coefficients. Predictions show that heavily loaded GFBs comprising two bump layers in series and including stop pins prevent too large bump deflections which may induce permanent plastic deformations. The structural damping or loss factor in a GFB with a two bump strip layer enhances the bearing direct damping force coefficients.

INTRODUCTION

Oil-free micro turbomachinery requires of reliable gas foil bearing supports to ensure low friction and rotordynamic stability, along with the ability to sustain large loads, static and dynamic [1]. Bump foil GBs appear as an established technology for ready use even in power generation gas turbines [1]. The proper design, construction and operation of the FB compliant structure are of utmost importance. Walowit et al. [2] report evidence of permanent deformation of a bump foil strip in the most loaded zone during high-speed rub tests. Heshmat [3] introduces a multi-stage GFB with a double bump layer to increase the bearing structural stiffness and demonstrates a large load capacity, i.e. specific pressure of 6.7 bar (100 psi) at a rotor speed of 60 krpm. The same author [3] also shows stable operation of a GFB at 132 krpm (4.62×10^6 DN). Peng and Khonsari [4] introduce an analysis for the ultimate load capacity of a GFB operating at very high speeds, infinite in theory; and with results indicating that GFBs have a larger load capacity than a rigid surface bearing at a 20 μm ad-hoc minimum film thickness. Not only the minimum film determines the maximum load capacity, but most importantly, the maximum elastic deflection in the support structure (before yielding) dictates the actual load limit. Kim and San Andrés [5] verify analytically the performance of a heavily loaded test GFB which has an operating journal eccentricity over three times larger the nominal radial clearance in the bearing. At the load limit condition, the predictions show a nearly constant GFB static stiffness, indifferent to rotor speed, and in magnitude close to the foil support structural stiffness determined upon contact conditions without rotor spinning.

This paper presents an analysis of the static and dynamic forced performance of a GFB with piecewise linear elastic support. The double bump layer, as shown in Figure 1, consists of an upper *soft* bump strip and a lower *stiffer* bump strip (or stop pin). For simplicity, K_{f1} and K_{f2} represent the local stiffness/unit area. The bottom structure acts when the GFB is to support heavy loads (above a designed threshold), thus stiffening the local foundation, i.e. $K_f=K_{f1}+K_{f2}$. Presently, the computational model given in [5] is enhanced to model GFBs with piecewise linear elastic supports. Model predictions for a double strip layer GFB are compared to those for a single bump layer GFB.
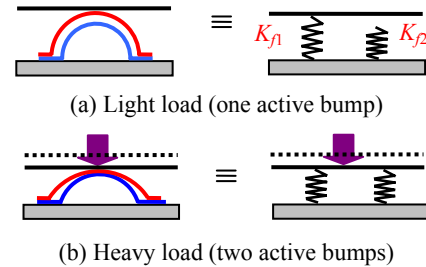

(a) Light load (one active bump)

(b) Heavy load (two active bumps)

Fig. 1 Equivalent elastic model for a double bump layer GFB.

ANALYSIS

The Reynolds equation for an isothermal, isoviscous (μ) gas describes the generation of the hydrodynamic pressure (p) within a film of thickness (h),

$$\frac{\partial}{\partial x}\left(ph^3 \frac{\partial p}{\partial x}\right) + \frac{\partial}{\partial z}\left(ph^3 \frac{\partial p}{\partial z}\right) = 6\mu\Omega R \frac{\partial(ph)}{\partial x} + 12\mu \frac{\partial(ph)}{\partial t} \qquad (1)$$

in $\{0<x<2\pi R, \ 0<z<L\}$ with Ω as the journal speed. The motion of the journal with small amplitude motions (Δe_X, Δe_Y) at frequency (ω) about equilibrium position (e_{X0}, e_{Y0}) is

$$e_X = e_{X0} + \Delta e_X e^{i\omega t}, \qquad e_Y = e_{Y0} + \Delta e_Y e^{i\omega t} \qquad (2)$$

Superposition of a zeroth order and perturbed (first-order) pressure fields follows as

$$p = p_0 + \Delta e_X \, p_X e^{i\omega t} + \Delta e_Y \, p_Y e^{i\omega t} \qquad (3)$$

The film thickness (h) for an <u>active</u> double bump layer is

$$h = h_0 + \Delta h e^{i\omega t} \qquad (4)$$

$$h_0 = c - r_p \cos(\Theta - \Theta_p) + e_{X0}\cos(\Theta) + e_{Y0}\sin(\Theta) + \frac{\delta p_{A0} + K_{f2} \cdot w_f}{K_{f1} + K_{f2}};$$

$$\Delta h = \Delta e_X \cos(\Theta) + \Delta e_Y \sin(\Theta) + \frac{\Delta e_X \delta p_{AX} + \Delta e_Y \delta p_{AY}}{(K_{f1} + K_{f2})(1+i\gamma)};$$

$$\delta p_{A0} = \frac{1}{L}\int_0^L (p_0 - p_a)dz; \quad \delta p_{AX} = \frac{1}{L}\int_0^L p_X dz; \quad \delta p_{AY} = \frac{1}{L}\int_0^L p_Y dz$$

c, r_p, are the nominal clearance and assembly preload; p_a is the ambient pressure and δP is an axially averaged pressure acting on the foil. The structural loss factor (γ) models the energy dissipation arising from the relative motion between top foil and bumps, for example. The lower bump becomes active when the local pressure pushes the upper bump beyond a *critical* elastic deflection, $w_f = H_{B1} - T_{B1} - H_{B2}$, where H_{B1} and H_{B2} are the heights of the upper and lower bump strips, and T_{B1} is the thickness of the upper bump. In Eqn. (4), setting $K_{f2} = 0$ gives the film thickness for a single bump layer and local deflection $w_d = \delta p_{A0}/K_{f1}$ $< w_f$. Substituting Eqns. (3, 4) into (1) leads to zeroth- and first- order equations for the equilibrium and perturbed pressure fields; and whose solution is obtained numerically using an advanced flow advection model [5]. Integration of the equilibrium and perturbed pressures on

the bearing surface renders the GFB reaction forces and frequency dependent stiffness and damping force coefficients.

RESULTS AND DISCUSSION

Model predictions follow for a test GFB with a nominal clearance (c) of 31.8 μm, determined from the recorded journal radial travel in a small load-deflection test without rotor spinning [6]. The original GFB, with $L=D$=38.1 mm, has a single bump layer, with dimensionless compliance $S_l = p_a/(cK_{fl})$ = 0.67. Presently, a second bump layer of identical stiffness ($K_{f2}=K_{fl}$=4.74 GN/m^3) is located underneath the upper (original) layer. The bump thicknesses, $T_{Bl}=T_{B2}$ = 0.102 mm, with heights H_{Bl}=0.508 mm and H_{B2}=0.375 mm, determine a critical upper layer deflection, w_f, equal to 31 μm.

Figure 2 shows the predicted journal eccentricity and maximum bump structural deflection versus static load for three GFB configurations operating at 40 krpm. Single and double layer configurations are described above. Setting the compliance of the lower bump as nil, $S_2=p_a/(cK_{f2})$=0, denotes $K_{f2}\rightarrow\infty$, which represents a rigid stop pin. Note that the single bump layer GFB shows the largest journal motions ($> c$) and structural deflection due to the softness of its elastic structure. For loads above 150 N, the stop pin with same height as the lower bump layer prevents larger structural deflections and determines the smallest journal eccentricity. Note that the difference between maximum structural deflection and eccentricity is the minimum film thickness.

Figure 3 depicts the stiffness and damping coefficients versus excitation frequency (ω) for single and double bump layer GFBs operating at 40 krpm (667 Hz). A large load of 300 N along the X-direction activates the lower bumps of the double layer GFB, thus increasing significantly the bearing direct stiffness coefficients (K_{XX}, K_{YY}). The cross-coupled stiffnesses (K_{XY}, K_{YX}) also increase; thus requiring of a careful design for rotordynamic considerations. The structural loss factor, γ = 0.2, represents material hysteresis and dry-friction effects which are advantageous in GFBs. A double layer GFB shows an increased direct damping C_{XX} since both upper and lower layers are active. As with all gas bearings, the damping coefficients decrease in magnitude as the excitation frequency (ω) increases. Using Lund's model [7], one easily determines a whirl frequency ratio (WFR) equal to zero for operation with a static load larger than 50 N. Thus, at 40 krpm, both single and double layer GFBs should be rotor dynamically stable. When active, the stop pins eliminate the damping effect from the elastic foundation, thus making the operation vulnerable to instability.

CONCLUSIONS

The paper presents an analysis of GFB with multi-stage elastic supports. Predictions show that a double bump layer GFB or a GFB with stop pins supports a heavy load with a smaller journal eccentricity than that in a single bump layer GFB. The double-layer GFB renders larger direct stiffness and damping coefficients, further enhanced by the material hysteresis (structural loss). However, increased fabrication cost and complexity in assembly are disadvantages to be considered.

ACKNOWLEDGMENTS

REFERENCES

[1] DellaCorte, C., and Valco, M. J., 2000, "Load Capacity Estimation of Foil Air Journal Bearings for Oil-Free Turbomachinery Applications," Tribology Transactions, **43**(4), pp. 795-801.

[2] Walowit J., Murray, S. F., McCabe, J., Arwas, E. B., and Moyer, T., 1973, "Gas Lubricated Foil Bearing Technology Development for Propulsion and Power Systems," AFAPL-TR-73-92.

[3] Heshmat, H., 1994, "Advancements in the Performance of Aerodynamic Foil Journal Bearings: High Speed and Load Capacity," ASME J. of Tribology, **116**, pp 287-295.

[4] Peng, Z.-C., and Khonsari, M. M., 2004, "On the Limiting Load-Carrying Capacity of Foil Bearings," ASME J. of Tribology, **126**, pp 817-818.

[5] Kim, T.H, and San Andrés, L., 2005, "Heavily Loaded Gas Foil Bearings: a Model Anchored to Test Data," ASME Paper GT2005-68486.

[6] Ruscitto, D., Cormick, J. Mc., and Gray, S., 1978, "Hydrodynamic Air Lubricated Compliant Surface Bearing For An Automotive Gas Turbine Engine I-Journal Bearing Performance," NASA CR-135368

[7] Lund, J. W., 1968, "Calculation of Stiffness and Damping Properties of Gas Bearings," ASME J. of Lubrication Technology, **90**, pp 793-803.
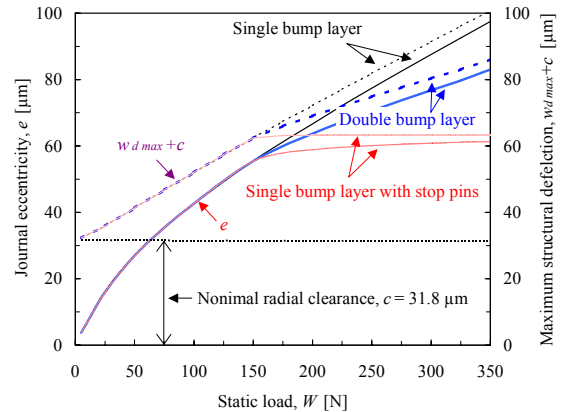

Fig. 2 Journal eccentricity and maximum structural deflection vs. static load for GFB with (a) single bump layer, (b) double bump layer, and (c) single bump layer with stop pin. Journal speed = 40 krpm. Compliance parameters: $S_{1,2}$= 0.67 for (a) & (b); S_2 = 0 for (c).
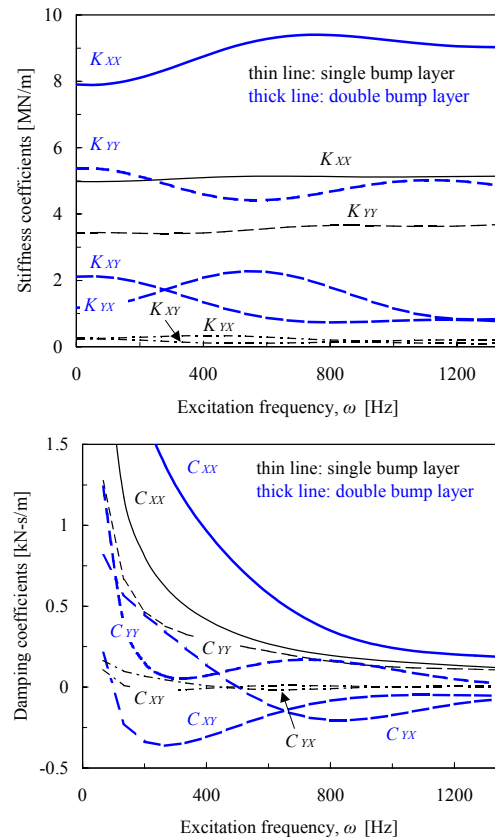

Fig. 3 Stiffness and damping coefficients versus excitation frequency for single and double bump layer GFBs at 40 krpm (667 Hz). Static load: 300 N. Compliance parameters $S_{1,2}$ = 0.67, loss factor γ=0.2